© IIJP 2025 | Volume 1, Issue 3, pp.402-417 | ISSN: 2636-4484

NUMERICAL INVESTIGATION OF MAGNETOHYDRODYNAMIC FLOW IN A VERTICAL CHANNEL FILLED WITH POROUS MEDIA UNDER THE COMBINED INFLUENCE OF THERMAL RADIATION, VISCOUS DISSIPATION AND TEMPERATURE-DEPENDENT VISCOSITY

Yusuf A.B[1], Suleiman U.[2] & Suleiman S.[3]

[1,2&3]*Department of Mathematics, Federal University Dutsin-Ma*

Corresponding Author: Suleiman U/*Email: umarsuleiman3355@gmail.com*

ARTICLE INFO

Article No.: 051

Accepted Date: 20/08/2025

Published Date: 09/09/2025

Type: Research

ABSTRACT

This study numerically investigates the magneto hydrodynamics (MHD) flow in a vertical porous channel filled with porous materials considering the joint influence of thermal radiation, viscous dissipation and temperature dependent viscosity. The governing equation are transformed in to dimensionless equation then are solved numerically using Runge Kutta Order Four with Shooting techniques by using MATLAB package. The effect of pertinent parameters on flow characteristics, temperature distribution and velocity profiles are analyzed. The results provide insights into the complex interactions between magnetic fields, thermal radiation and viscous dissipation in a porous media, with potential applications in fields like geothermal energy, nuclear reactors and thermal insulation. The findings highlight the significance of considering temperature dependent viscosity and thermal radiation in MHD flow through porous channels.

Keywords: Magnetohydrodynamic (MHD) flow, Vertical porous channel, Porous materials, Thermal radiation, viscous dissipation, Temperature-dependent viscosity, Runge-Kutta fourth order

.

Introduction

Magnetohydrodynamics (MHD) explores the interaction between electrically conductive fluids such as plasmas, liquid metals, saltwater and magnetic fields. This field of research combines principles from electromagnetism, fluid dynamics and thermodynamics. MHD fluids are distinguished by the presence of electrically charged particles, including ions and electrons that can move freely within the fluid. These fluids possess distinctive properties, including: Its ability to conduct electricity due to presence of charged particles, (electrical conductivity). Its ability to interact with magnetic fields, which can induce electric currents and forces within the fluid, (Magnetic field interaction). And that it can exhibits complex flow behavior, including turbulence, waves and instabilities, (Complex flow behavior). MHD flow has widespread applications in manufacturing and industry, including system cooling, MHD generators, accelerators, nuclear reactors, pumps, geothermal energy extraction, energy storage, and furnace structures. It also has many applications in biomedical engineering which is used to facilitate curing fracture in bones, blood flow and in dealing with some other various pathological situations.

Numerous studies have investigated the Magnetohydrodynamic (MHD) flow in vertical channels filled with porous media, considering various factors such as thermal radiation, viscous dissipation, and temperature-dependent viscosity. Here are some key findings: Thermal radiation has significantly impacts on MHD flow in vertical channels. For instance, Venkateswara Reddy Malapati and P Bhaskar (2021) studied the influence of heat generation and thermal radiation on MHD flow in a vertical micro-porous channel, highlighting the importance of thermal radiation in such flows. Viscous dissipation is another crucial factor in MHD flow. Studies by Abbas et al. (2023) and Mishra and Kumar (2020) demonstrated the significance of viscous dissipation in MHD nanofluid flow and heat transfer over a vertical cone and stretching sheet, respectively. Temperature-dependent viscosity is a critical aspect of MHD flow. Pandit et al. (2022) investigated the effect of thermal radiation and suction/injection on MHD convective flow with viscous dissipation, highlighting the importance of temperature-dependent viscosity in such flows. Temperature-dependent viscosity has an effects on fluid behavior and heat transfer Kumar et al., (2018). Research has shown that temperature-dependent viscosity alters velocity profiles and flow rates (Saha et al., 2020) and interacts with thermal radiation and viscous dissipation Nield & Bejan, (2017). Sinha and Choudhury (2024) investigated unsteady MHD flow from a vertical porous plate with heat source, highlighting the effects of thermal radiation and viscous dissipation. Kodi et al. (2022) examined MHD mixed convection flow along a cone embedded in a porous medium with variable surface temperature, emphasizing the significance of porous media in MHD flow.

Magneto hydrodynamics (MHD) flow in porous channels has garnered significant attention due to its applications in various fields, including geothermal energy Kumar et al., (2018), nuclear reactors Saha et al.,(2020), and thermal insulation Nield & Bejan, (2017). MHD flow in porous media has been extensively studied, with researchers exploring various aspects, such as flow characteristics (Al-Nimr & Alkam, 2000), heat transfer (Chamkha, 2001), and mass transfer (El-Amin, 2004). Studies have shown that MHD flow in porous channels is significantly influenced by magnetic field strength (Raptis et al., 2003), porous medium properties (Nield & Bejan, 2017), and fluid properties (Kumar et al., 2018).

Thermal radiation plays a crucial role in MHD flow, particularly in high-temperature applications (Hossain & Takhar, 1996). Research has shown that thermal radiation enhances heat transfer rates (Raptis et al., 2003) and interacts with other parameters, such as magnetic field strength and viscous dissipation (Saha et al., 2020). Viscous dissipation is another important factor in MHD flow, as it generates heat due to fluid friction (Gebhart, 1962). Studies have demonstrated that viscous dissipation affects velocity profiles and flow rates

(Al-Nimr & Alkam, 2000) and enhances temperature distribution (Chamkha, 2001). Recent studies have explored various aspects of MHD flow in porous channels, including: MHD flow with heat generation: Saha et al. (2020) investigated MHD flow with heat generation and thermal radiation. MHD flow with variable viscosity: Kumar et al. (2018) studied MHD flow with variable viscosity and thermal conductivity.

Despite the extensive research on MHD flow in vertical channels with porous media, there is still a need for further investigation into the combined effects of thermal radiation, viscous dissipation, and temperature-dependent viscosity on MHD flow. Specifically, the interaction between these factors and their impact on flow characteristics, heat transfer, and mass transfer requires more attention.

The objective of this article is to numerically investigate the MHD flow in a vertical channel filled with porous media under the combined influence of thermal radiation, viscous dissipation, and temperature-dependent viscosity. The study aims to:

1. Analyze the impact of thermal radiation, viscous dissipation, and temperature-dependent viscosity on MHD flow characteristics
2. Examine the effects of these factors on heat transfer and mass transfer
3. Provide insights into the interaction between these factors and their significance in MHD flow applications

This review focuses on the numerical investigation of MHD flow in a vertical porous channel filled with porous materials, considering the joint influence of thermal radiation, viscous dissipation, and temperature-dependent viscosity.

This paper is an extension of the published paper by Yusuf A.B and Abiodun O.A (2018)

Mathematical formulation

Figure 1 below illustrates the schematic diagram of the problem, depicting two infinitely parallel plates separated by a distance h, forming a vertical channel. It is assumed that all fluid properties remain constant except for viscosity and thermal conductivity, which depend entirely on time. Additionally, the fluid flow is influenced by a magnetic field B_0 and gravitational force g. The flow is directed vertically upward along the $x-axis$,while measurements are taken perpendicular to the plates along the $y-axis$. The temperature of the plate at $y=0$ is initially increased to T_w and then maintained constant, whereas the opposite plate at $y'=h$ remains stationary at temperature T_0.

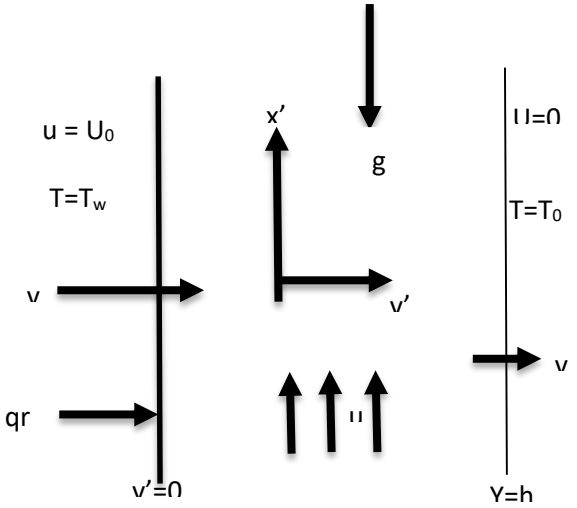

Figure 1: schematic diagram of the problem

Under these assumptions, the appropriate governing equations adopted in Yusuf, A.B. and Abiodun O. A. (2018) are:

$$\frac{\partial u}{\partial t} + \nu \frac{\partial u}{\partial y'} = \frac{1}{\rho}\frac{\partial}{\partial y'}\left(\mu_{eff}\ \frac{\partial u}{\partial y'}\right) + g\beta(T - T_0) - \frac{\mu u}{K} + \frac{\delta B_0^2 U}{\rho} \quad (1)$$

$$\frac{\partial T}{\partial t} + \nu \frac{\partial T}{\partial y'} = \alpha\left(\frac{\partial^2 T}{\partial y'^2} + \frac{1}{k}\frac{\partial q_r}{\partial y'}\right) + \frac{\mu}{\rho c_p}\left(\frac{\partial u}{\partial y'}\right)^2 \quad (2)$$

Where q_r is defined below:

$$q_r = \frac{-4\sigma}{3\delta}\frac{\partial T^4}{\partial y'} \quad (3)$$

with the boundary condition

$$\begin{aligned} &u = U_0, \quad T = T_{w,} \quad \text{at} \quad y' = 0 \\ &u = 0, \quad T = T_{0,} \quad \text{at} \quad y' = h \end{aligned} \quad (4)$$

Equation (1) represent the momentum equation in which first and second term in LHS represent velocity gradient with respect to time, fluid velocity due to suction, with first, second, third and fourth term in RHS represent variable viscosity effect, buoyancy force, Velocity of fluid due to porous channel and joule heating respectively. Equation (2) represent the energy equation where first and second term in LHS representing rate of change of temperature with time, heat due to fluid suction and first, second, and third terms in RHS representing conductive heat transfer in y-direction, thermal conductivity due to thermal radiation Equation, viscous dissipation effect correspondingly. Equation (3) represent the radiative heat flux, Equation (4) represent the boundary conditions respectively.

Non-dimensionalization of the problem

In order to transform the governing equations into dimensionless form, the following similarity variables are adopted in Yusuf, A.B. and Abiodun O. A. (2018) are utilized.

$$U = u_0 f(y), \quad y = \frac{y'}{\sqrt{\nu t,}}, \quad \mu = \mu_0\left(1 - \lambda\theta(y)\right), \quad \delta = 2\sqrt{\nu t}, \quad \frac{\partial T}{\partial y} = \theta'(y)(T_w - T_0) \quad (5)$$

using equation (3) and (5) in (1) and (2) we obtained the following differential equations:

$$f''(y) = \left[\frac{-1}{2\Gamma}(y + c) - \lambda\theta'(y)\left(1 + \lambda\theta(y)\right)\right]f'(y) + \left[\frac{\left(1-\lambda\theta(y)\right)}{\Gamma Da} - \frac{M}{\Gamma}\right]f(y) - \frac{Gr\theta(y)}{\Gamma} \quad (6)$$

$$\theta''(y) = -\frac{1}{2}Pr(y + C)\theta'(y)\left[1 - \frac{4}{3}R[\theta(y) + \emptyset]^3\right] - 4R[\theta(y) + \emptyset]^2\theta(y)\left[1 - \frac{4}{3}R[\theta(y) + \emptyset]^3\right] - Br\,(f'(y))^2\left[1 - \frac{4}{3}R[\theta(y) + \emptyset]^3\right] \quad (7)$$

Where $\Gamma = \frac{\mu_{eff}}{\mu}$ $Gr = \frac{g\beta(T_w - T_0)\delta^2}{4U_0\upsilon}$ $Da = \frac{K}{\mu t}$ $M = \frac{\delta B_0^2 t}{\rho}$ $\emptyset = \frac{T_0}{T_w - T_0}$

$C = \frac{\upsilon t^{\frac{1}{2}}}{\sqrt{\upsilon}}$ $Pr = \frac{\upsilon}{\alpha}$ $R = \frac{4\gamma(T_w - T_0)^2}{K\delta}$, $\theta(y) = \frac{T - T_0}{T_w - T_0}$, $J = M_n P_r$ (8)

Similarly, the boundary conditions on using (6) and (7) are now:

$f(0) = \theta, (0) = 1$ at $y = 0$ (9)

$f(H) = \theta(H) = 0$ at $y = 1$ (10)

Methodology of solution

Mathematical description of RK4 with shooting method

The Runge-Kutta fourth order method (RK4) is a numerical technique for solving ordinary differential equations (ODEs). When applied alongside the shooting method, it becomes useful for solving boundary value problems (BVPs).

Here's a mathematical description of the RK4 method with the shooting method:

Step 1: Define the ODE and boundary conditions

Given an ODE of the form:

$\frac{dy}{dx} = f(x, y)$

With boundary conditions:

$y(x = a) = ya$

$y(x = b) = yb$

Step 2: Discretize the interval $[a, b]$

Divide the interval $[a, b]$ into N equal subintervals, with step size $h = \frac{b-a}{N}$

Step 3: Define the shooting method parameters

Choose an initial guess for the unknown initial condition, $y(a)$ as y_0

Step 4: Implement the RK4 method

Using the RK4 method, approximate the solution of the ODE at each interior point, $x_i = a + ih$, as follows:

$$k_1 = h * f(x_i, y_i)$$
$$k_2 = h * f(x_i + 0.5h, y_i + 0.5k_1)$$
$$k_3 = h * f(x_i + 0.5h, y_i + 0.5k_2)$$
$$k_4 = h * f(x_i + h, y_i + k_3)$$
$$y_{(i+1)} = y_i + \left(\frac{1}{6}\right)(k_1 + 2k_2 + 2k_3 + k_4)$$

The choice of this method is due to the higher complexity of the governing equations. The advantages of this method are it provides high accuracy, flexible to handle and its robustness.

Result and Discussion of the problem

This study investigates the effects of temperature-dependent viscosity, viscous dissipation and thermal radiation on the flow characteristics of MHD fluid through a vertical porous channel. The key parameters considered include varying viscosity ($\boldsymbol{\lambda}$), suction parameter (c), magnetic parameter (M), Darcy number (Da), Prandtl number (Pa), and Grashof number (Gr). The model equations are simulated using MATLAB. Specifically, the selected values for (M), (Da), ($\boldsymbol{\lambda}$), and (Br) are as follows: (2.50, 3.00, 3.50, 2.90, 1.90),

(0.50, 1.00, 1.50, 2.00, 2.50), (0.20, 0.40, 0.60, 0.80, 1.00) and (0.10, 0.50, 1.00, 2.50, 3.50) respectively. Results of these simulations are displayed on graphs and discussed below.

Graphical Representation of the Results and discussion

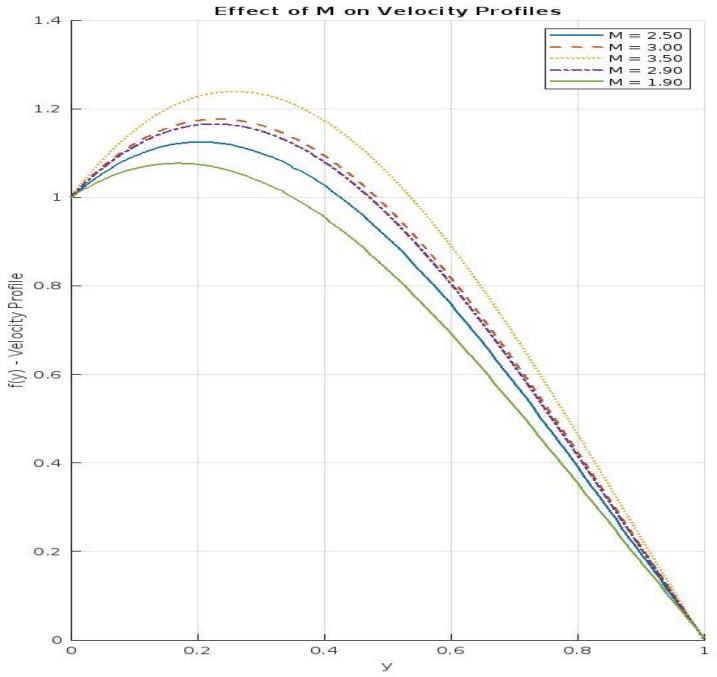

Figure 2. Effect of M on Velocity profile

$$M = \{2.50, 3.00, 3.50, 2.90, 1.90\};\ Da = 0.75, Pr = 0.8, Br = 1,\ \Gamma = 1.5,$$

$$Phi = 0.5,\ \ R = 0.5, \boldsymbol{\lambda} = 0.6, Gr = 10,$$

Figure 2 illustrates the velocity distribution for various values of (M). The figure reveals that as M increases, the fluid velocity also increases accordingly. A higher magnetic parameter can lead to a more uniform velocity profile. The statements represent the influence of a magnetic field on the electrically conducting fluid. A higher magnetic parameter typically means a stronger magnetic field or higher electrical conductivity. Note M is the magnetic field parameter.

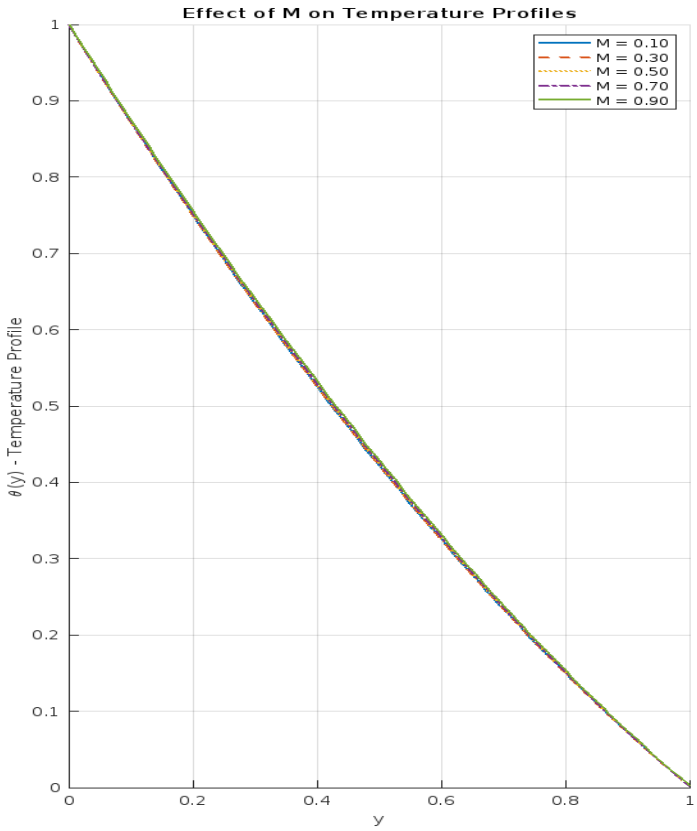

Figure 3. Effect of M on Temperature profile

$$M = \{2.50, 3.00, 3.50, 2.90, 1.90\};\ Da = 0.75, Pr = 0.8, Br = 1, \qquad \Gamma = 1.5,$$

$$Phi = 0.5,\ \ R = 0.5,\ \boldsymbol{\lambda} = 0.6, Gr = 10,$$

Figure 3 depicts the temperature distribution for different values of (M). The figure indicates that as M increases, the fluid temperature also rises. In a conducting fluid, an increase in M generates a magnetic force that interacts with the fluid flow, leading to a temperature increase. The statement describes a thermal effect that occurs in Magnetohydrodynamic (MHD) flows, where conducting fluid moves in the presence of a magnetic field. Normally a higher magnetic parameter strengthens magnetic forces within the fluid. These forces resist motion, which leads to more dissipation of energy as heat (via joule heating). As a result, the fluids temperature increases. This phenomenon is essential in industrial applications involving liquid metals, MHD generators or plasma containment, where balancing magnetic control and thermal effects is key.

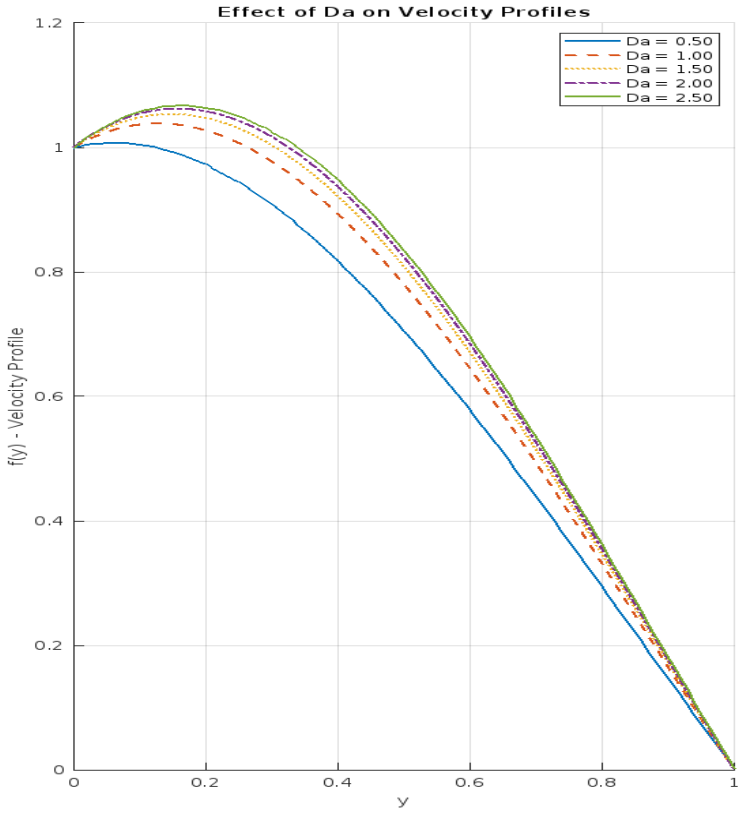

Figure 4. Effect of Da on Velocity

$$Da = \{0.50, 1.00, 1.50, 2.00, 2.50\};\ Pr = 0.75, c = 0.2, Br = 0.9,\ \Gamma = 1.5,$$

$$Phi = 0.2,\ R = 0.4,\ \boldsymbol{\lambda} = 0.3, Gr = 5,\ M = 1.5$$

Figure 4 illustrates the velocity distribution for various values of (Da). The figure shows that as Da increases, the fluid velocity also increases. A higher Da value can enhance the reaction, generating momentum and energy, which contributes to the rise in fluid velocity. When darcy parameter increases, it implies that the permeability of the medium increases, allowing for easier fluid flow.

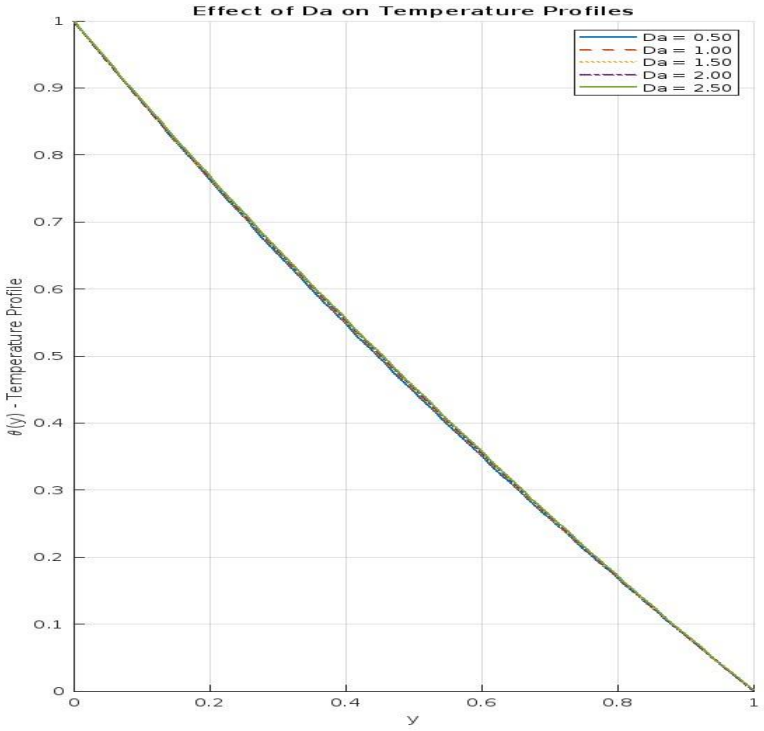

Figure 5. Effect of Da on Temperature profile

$$Da = \{0.50, 1.00, 1.50, 2.00, 2.50\};\ Pr = 0.75, c = 0.2, Br = 0.9,\ \ \Gamma = 1.5,$$

$$Phi = 0.2,\ \ R = 0.4, \boldsymbol{\lambda} = 0.3, Gr = 5,\ M = 1.5$$

Figure 5 presents the temperature distribution for various values of (Da). The figure indicates that as Da increases, the fluid temperature also rises. Higher Da values indicate increased permeability, allowing for more efficient fluid flow and convective heat transfer. This can lead to a more uniform temperature profile.

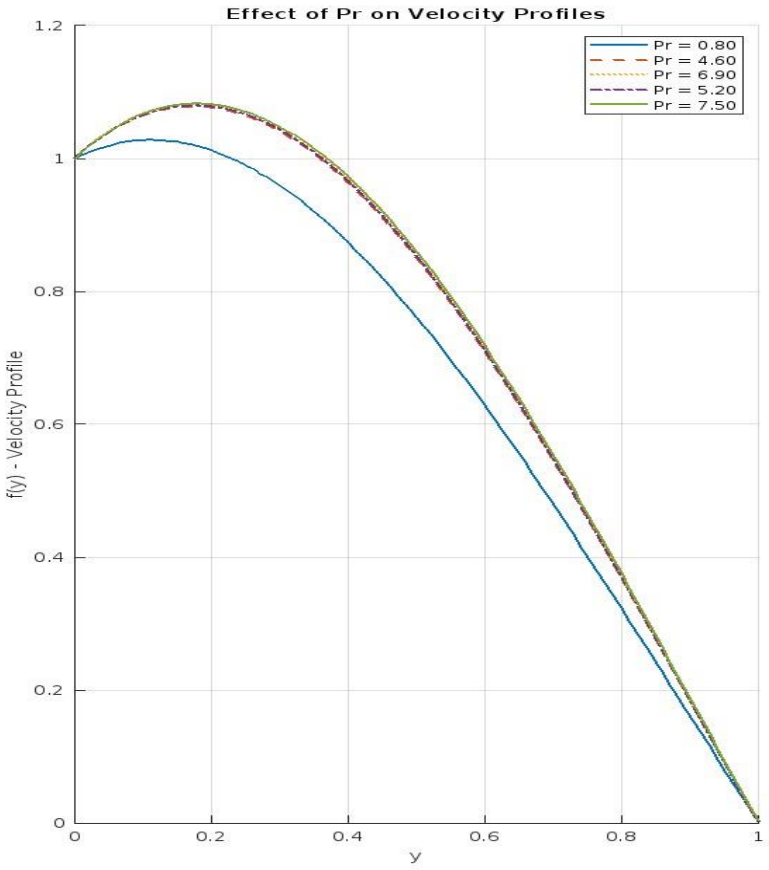

Figure 6 Effect of Pr on Velocity profile

$$Pr = \{0.80, 4.60, 6.90, 5.20, 7.50\};\ \boldsymbol{\lambda} = 0.2, c = 0.1, Br = 0.5, \Gamma = 1.0,$$

$$Phi = 0.2,\ \ R = 0.3,\ \ Da = 0.71, Gr = 5,\ \ M = 1.0$$

The impact of Pr is shown in Figure 6. It is observed that as Pr increases, the fluid velocity within the channel decreases. This occurs because a higher Pr value weakens the convection currents of the fluid molecules, which is a result of the temperature reduction.

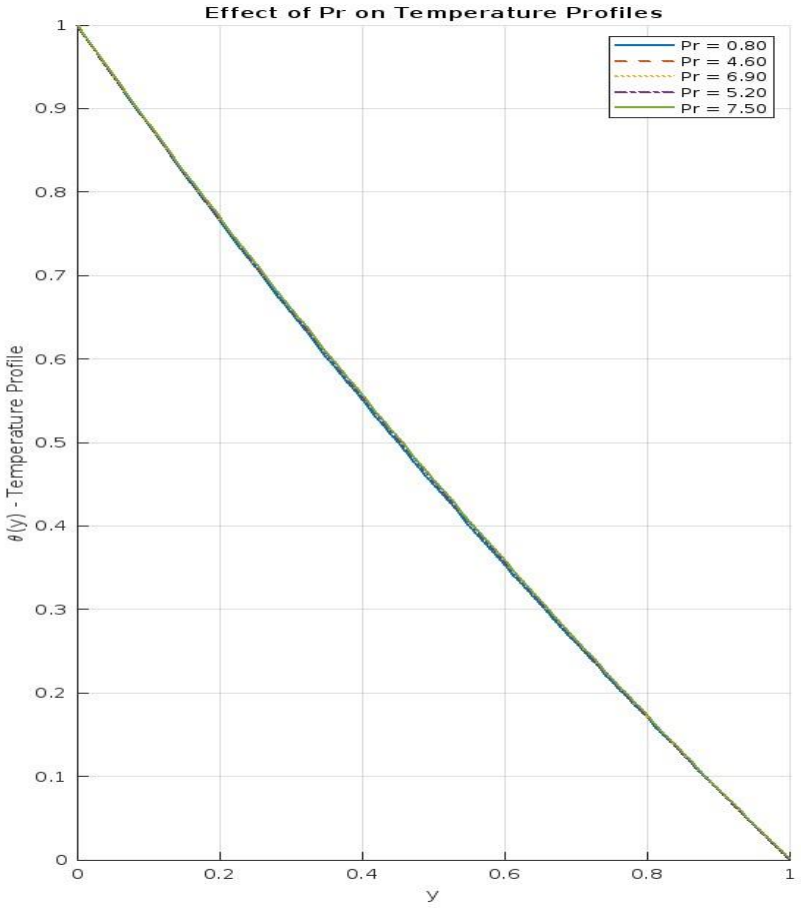

Figure 7 Effect of Pr on Temperature profile

$$Pr = \{0.80, 4.60, 6.90, 5.20, 7.50\};\ \boldsymbol{\lambda} = 0.2, c = 0.1, Br = 0.5, \Gamma = 1.0,$$

$$Phi = 0.2,\ \ R = 0.3,\ \ Da = 0.71, Gr = 5,\ \ M = 1.0$$

Figure 7 illustrates the impact of the Prandtl number (Pr) on fluid temperature. The figure shows an inverse relationship between fluid temperature and Pr, meaning that as Pr increases, thermal diffusion within the channel decreases, leading to a reduction in heat flux.

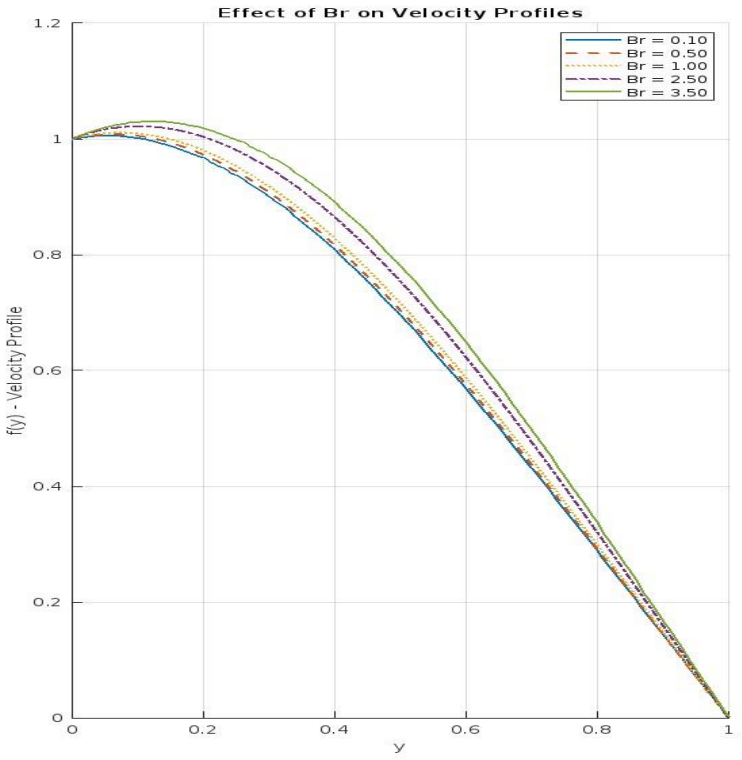

Figure 8 Effect of Br on Velocity

$$Br = \{0.10, 0.50, 1.00, 2.50, 3.50\};\ Pr = 0.71, c = 0.1, \boldsymbol{\lambda} = 0.2, \Gamma = 1.0,$$

$$Phi = 0.2,\ \ R = 0.3,\ Da = 0.50, Gr = 5.0,\ M = 1.0$$

Figure 8 illustrates the velocity distribution for various values of Br. The figure shows that as Br increases, the fluid velocity decreases.

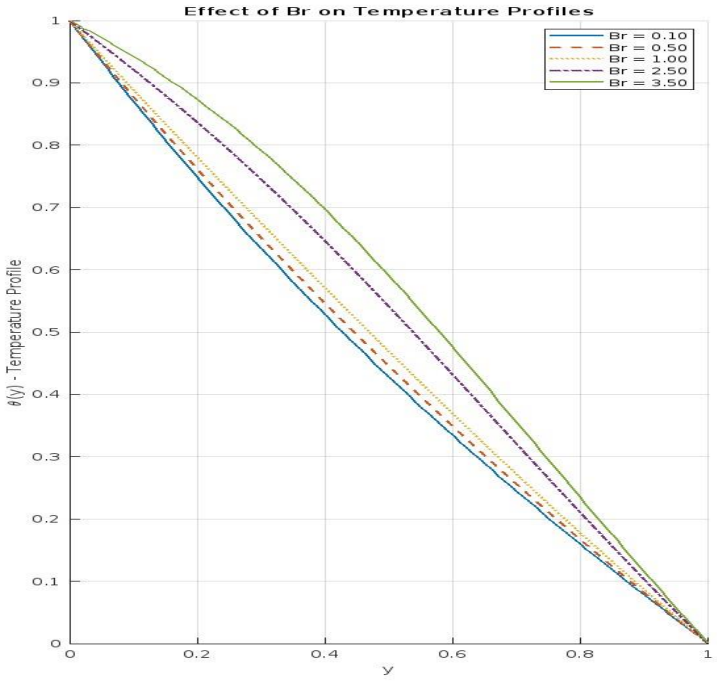

Figure 9 Effect of Br on Temperature profile

$Br = \{0.10, 0.50, 1.00, 2.50, 3.50\};\ Pr = 0.71, c = 0.1, \boldsymbol{\lambda} = 0.2, \Gamma = 1.0,$
$Phi = 0.2,\ \ R = 0.3,\ \ Da = 0.50, Gr = 5.0,\ \ M = 1.0$

Figure 9 shows the temperature distribution for different values of Br. It can be seen from the figure that, an increase in Br results into a corresponding increase in velocity of the fluid.

Table 1: Computed values of skin friction on the walls for the Problem.

Pr	$Da = 0.1, c = 0.1, \lambda = 0.2, \Gamma = 1,$ $\phi = 0.2, Br = 0.5, R = 0.3, M = 1,$ $Gr = 5$		$Da = 0.8, c = 0.1, \lambda = 0.2, \Gamma = 1,$ $\phi = 0.2, Br = 0.5, R = 0.3, M = 1,$ $Gr = 5$	
	τ_0	τ_1	τ_0	τ_1
1.0	-1.59900	-0.62692	0.50744	-1.55910
2.0	-1.62380	-0.59576	0.46048	-1.50290
3.0	-1.64780	-0.56692	0.41506	-1.45040
4.0	-1.67090	-0.54052	0.37160	-1.40190
5.0	-1.69290	-0.51659	0.33041	-1.35750

Table 1 presents the effects of varying Pr on skin friction. The table indicates that skin friction between the channel walls and the working fluid decreases at y = 0 as Pr increases, while it increases at y = 1 with rising Pr. Additionally, it is observed that skin friction at y = 0 decreases with increasing Da, whereas it increases at y=1 as Da increases, with other parameters held constant.

Table 2: Numerical data for the heat transfer rate along the channel walls of the Problem

Pr	$Da = 0.1, c = 0.1, \lambda = 0.2, \Gamma = 1,$ $\phi = 0.2, Br = 0.5, R = 0.3, M = 1,$ $Gr = 5$		$Da = 0.8, c = 0.1, \lambda = 0.2, \Gamma = 1,$ $\phi = 0.2, Br = 0.5, R = 0.3, M = 1,$ $Gr = 5$	
	NU_0	NU_1	NU_0	NU_1
1.0	1.33830	0.72710	1.26470	0.76525
2.0	1.43720	0.59995	1.36410	0.63278
3.0	1.53760	0.49113	1.46510	0.51917
4.0	1.63880	0.39904	1.56710	0.42284
5.0	1.74000	0.32195	1.66900	0.34205

Table 2 presents the impact of the Prandtl number (Pr) on the heat transfer rate between the channel walls and the working fluids. It was observed that the Nusselt number, representing the heat transfer rate, increases with rising Pr at $y = 0$ but decreases as Pr increases at the wall located at $y = 1$. Additionally, the Nusselt number at $y = 0$ increases with Darcy number (Da), whereas at $y = 1$, it decreases as Da increases.

Summary of the Work

In this study, one problem model was formulated based on the schematic representation of the problem and the fluid flow formation. These models were initially derived in their dimensional form and later transformed into a non-dimensional form using appropriate scaling parameters. The solutions were obtained using the Runge-Kutta fourth-order (RK4) method combined with the shooting technique. MATLAB, a computer algebraic package, was utilized for simulations and the results were presented graphically along with their discussions.

Conclusion

This research examined MHD natural convection flow in a vertical porous channel filled with porous materials. In this paper the model focused on temperature-dependent viscosity, thermal conductivity and viscous dissipation in MHD natural convection flow within the same channel setup.

The key findings of the paper are as follows:

(i)A rise in viscosity leads to a reduction in velocity and also lowering the fluid temperature.

(ii) Fluid suction results in a decrease in both velocity and temperature within the channel.

(iii) A stronger magnetic effect improves the velocity of the fluid.

(iv) A higher Brinkman number causes an increase in both velocity and temperature profiles.

References

Abbas, W., et al. (2023). Numerical Analysis of MHD Nanofluid Flow Characteristics with Heat and Mass Transfer over a Vertical Cone Subjected to Thermal Radiations and Chemical Reaction.

Al-Nimr, M. A., & Alkam, M. K. (2000). MHD forced convection flow in an open-ended parallel-plate channel. Heat and Mass Transfer, 36(2), 141-148.

Chamkha, A. J. (2001). Hydromagnetic combined convection flow in a vertical channel. International Journal of Engineering Science, 39(12), 1357-1374.

El-Amin, M. F. (2004). Combined effect of viscous dissipation and Joule heating on MHD flow past a semi-infinite inclined plate. Journal of Magnetism and Magnetic Materials, 270(1-2), 171-181.

Gebhart, B. (1962). Effects of viscous dissipation in natural convection. Journal of Fluid Mechanics, 14(2), 225-232.

Hossain, M. A., & Takhar, H. S. (1996). Radiation effect on mixed convection along a vertical plate with uniform surface temperature. Heat and Mass Transfer, 31(4), 243-248.

Kumar, P., Mahato, G. K., & Kumar, R. (2018). MHD flow of a variable viscosity fluid through a porous medium. Journal of Porous Media, 21(10), 931-943.

Kodi, R., et al. (2022). Periodic magnetohydrodynamic mixed convection flow along a cone embedded in a porous medium with variable surface temperature.

Mishra, A., & Kumar, M. (2020). Thermal Performance of MHD Nanofluid Flow Over a Stretching Sheet Due to Viscous Dissipation, Joule Heating and Thermal Radiation.

Nield, D. A., & Bejan, A. (2017). Convection in porous media. Springer.

Pandit, K. K., et al. (2022). EFFECT OF HEAT AND MASS TRANSFER AND THERMAL RADIATION ON A STEADY MHD CONVECTIVE FLOW WITH VISCOUS DISSIPATION AND SUCTION/INJECTION

Sinha, A., & Choudhury, L. (2024). MHD Flow from a Vertical Porous Plate in Presence of Heat Source.

Venkateswara Reddy Malapati, & P Bhaskar. (2021). Influence of Heat Generation and Thermal Radiation on MHD Flow in a Vertical Micro-Porous-Channel in the Presence of Viscous Dissipation

Raptis, A., Perdikis, C., & Takhar, H. S. (2003). Effect of thermal radiation on MHD flow. International Journal of Heat and Mass Transfer, 46(14), 2713-2716.

Yusuf, A.B. and Abiodun O. A. (2018) Unsteady natural convection flow through a vertical porous channel filled with porous materials under the effect of thermal radiation *FUDMA Journal of Sciences (FJS)* Vol. 2 No. 2, June, pp 102 - 115

Nomenclature and Greek symbol

Symbol	Interpretation	Unit
Gr	Grashof number	Non-dimensional
Pr	Prandtl number	Non-dimensional
Da	Darcy number	Non-dimensional
Γ	Viscosity ratio	Non-dimensional
c	Suction parameter	Non-dimensional
q_r	Radiative heat flux	Wm^{-2}
g	Gravitational acceleration	ms^{-2}
T	Dimensionless time	s
U_0	wall velocity	ms^{-1}
T_w	Wall temperature	K
T_0	Initial temperature of the fluid	K
h	Channel width	m
U	Dimensional velocity	ms^{-1}
Y	Dimensionless horizontal coordinate	Dimensionless
T	Dimensionless fluid temperature	K
k	Thermal conductivity of fluid	W/mk
K	Porosity of the porous media	m
u, v	Dimensionless velocity of the fluid	ms^{-1}

Greek symbols

Symbol	Interpretation	Unit
α	Thermal diffusivity	m^2s^{-1}
γ	Kinematic viscosity of the fluid	
γ_{eff}	Kinematic viscosity due to porous medium	
σ	Stefan – Boltzmann constant	Jk^{-1}